11th World Congress on Computational Mechanics (WCCM XI)
5th European Conference on Computational Mechanics (ECCM V)
6th European Conference on Computational Fluid Dynamics (ECFD VI)
E. Oñate, J. Oliver and A. Huerta (Eds)

DIRECT NUMERICAL SIMULATION OF FLOWS OVER A CAVITY WITH FLOW CONTROL USING A MOVING BOTTOM WALL

TAKASHI YOSHIDA*, TAKASHI WATANABE†

* Department of Environmental Science and Technology
Shinshu University
Wakasato 4-17-1, Nagano-shi, Japan
e-mail: yoshi-t@shinshu-u.ac.jp

† Graduate School of Information and Science
Nagoya University
Furo-cho, Chikusa-ku, Nagoya-shi, Japan
email: takashi@is.nagoya-u.ac.jp

Key Words: *Incompressible Flow, Direct Numerical Simulation, Cavity Flow Oscillation, Flow Control.*

Abstract. In this study, we investigate the control of self-sustained oscillating flows over an open cavity using a moving bottom wall. The three-dimensional incompressible Navier-Stokes equations are solved by finite difference method. A series of direct numerical simulations is performed for a variety of the bottom wall velocity from 0.00 to -1.00 with a cavity length-to-depth ratio of 2.0. The results show that velocity fluctuations and pressure fluctuations are suppressed due to the shear stress on the bottom wall of the cavity by the moving bottom wall. The most effective condition of the bottom wall velocity is -0.34. The rms value of the vertical velocity fluctuation is reduced by 68.9% when the moving bottom wall velocity is -0.34. The control method using the moving bottom wall is proved to be useful to suppress self-sustained cavity oscillations.

1 INTRODUCTION

Flows over cavities occur in a wide variety of aerospace and engineering applications: the landing systems of aircrafts, sunroofs and windows of automobiles, and spaces between bullet train cars. The cavity flow is of interest, because the presence of cavity causes self-sustained oscillations of the separated shear layer by a complex feedback mechanism, despite its geometrical simplicity. Flow-induced cavity oscillations and the feedback mechanism have been classified by Rockwell and Naudascher [1] into fluid-dynamic and fluid-resonant mechanism. Incompressible flows such as low-Mach number air flows and low-speed water flows over a cavity are classified as fluid-dynamic oscillations. For this condition, the acoustic wavelength is much longer than the length of the cavity, so that pressure fluctuations propagate instantaneously to the upstream leading edge of the cavity. The feedback mechanism can be regarded as purely hydrodynamic.

It is well known that the primary frequency of shear layer oscillations varies with cavity length. Many experimental studies have been carried out for understanding characteristics of oscillation frequency variation [2, 3, 4]. Self-sustained oscillations appear when the cavity length is above the minimum length which is required for the onset of self-sustained oscillations. This oscillation regime is referred to as "shear layer mode". The Strouhal number decreases as the cavity length increases. At some cavity length the Strouhal number jumps to higher value. These modes before and after the jump are called mode II and mode III.

The suppression of cavity flow oscillations has received considerable attention in recent years. The control of cavity oscillations has been reviewed by Rowley and Williams [5] and Cattafesta et al. [6]. Numerous workers have used various control devices, such as piezoelectric flaps, pulsed blowing actuators, fixed fences, spoilers, and ramps. They reported the suppression of oscillations by the control of a separated shear layer using these devices.

We developed a new active control method for suppression of the open cavity flow oscillations in two-dimensional simulations [7]. We focused on the role of recirculation vortices in the cavity with shear layer oscillations. The interaction between recirculating flow field and shear layer oscillations has been neglected in most previous studies. Our control method was achieved to tangentially drive the bottom wall of cavity toward upstream direction with a constant velocity, which is similar to the lid-driven cavity flow problem[8]. The moving bottom wall produced shear stress in fluid and changed recirculating vortices in the cavity. We presented that our control method completely eliminated self-sustained oscillations of the open cavity flow in two-dimensional simulations.

In this paper, we apply our control method using a moving bottom wall to three-dimensional flow over an open cavity and demonstrate the effects of the control method by direct numerical simulations. A series of direct numerical simulations is performed for a variety of bottom wall velocity. We are concerned with the relationship between cavity shear layer oscillations and recirculating vortices in the cavity. We demonstrate that cavity oscillations are suppressed using our control method.

2 NUMERICAL PROCEDURE AND CONTROL METHOD

The governing equations are the three-dimensional, unsteady, incompressible Navier-Stokes equations and the equation of continuity in Cartesian coordinates. All variables are nondimensionalized using the cavity depth D and the freestream velocity U. These equations are integrated in time using the P2 pressure correction method by Armfield and Street [9]. The momentum equations are discretized using second order Adams-Bashforth method for convective terms and Crank-Nicolson method for diffusive terms. These equations are solved by the fractional step method to satisfy the solenoidal condition. The pressure correction term is used with Kim and Moin type boundary condition [10] in order to reduce projection error and recover second-order accuracy in time. The second order fully conservative finite difference scheme by Morinishi et al. [11] is used for the convective terms and the second order central difference scheme is used for the other terms.

A schematic of the computational domain and the coordinates is shown in Figure 1. The length-to-depth ratio of cavity is 2. The computational domain extends by $5D$ upstream from the cavity leading edge, $7D$ downstream of the trailing edge, $9D$ in the normal direction above the cavity, and $2D$ in spanwise direction. Nonuniform staggered grid systems, which

cluster node points in the boundary layer, shear layer, the cavity bottom, and cavity edges, are used for spatial discretization. This size of x-y plane is similar to that used in the two-dimensional simulations of Rowley et al. [12]. The number of grid points are $447 \times 202 \times 20$ in x, y, and z direction, respectively. The laminar Blasius boundary layer is specified in the inflow boundary. A free-slip condition is applied to the normal boundary. At the outflow boundary, we use the Sommerfeld radiation condition, which is also called the convective outflow condition. The convective velocity in this condition is set equal to the freestream velocity. This boundary condition allows vortices to smoothly pass across the computational domain. The Reynolds number based on the freestream velocity and the cavity depth is $Re_D = 6,000$. The boundary layer momentum thickness θ at the upstream cavity edge is 0.03205. The Reynolds number based on U and θ is $Re_\theta = 192.3$. This condition is similar to that of experiment by Knisely and Rockwell [2], where $Re_\theta = 190$.

Figure 2 shows the geometry of the cavity in x-y plane and the schematic of the control method. The bottom wall of the cavity is moved horizontally with a negative constant velocity, like a lid-driven cavity problem. The bottom wall moving velocity u_w is varied from -0.10 to -1.00. The initial condition of control case is the instantaneous flow field of no control case at $t = 660$ and the bottom wall of cavity is suddenly started with u_w at $t = 660$. To evaluate performance of our control system, the flow variables are monitored at a point A ($x = 6.9,\ \ y = 0.0,\ z = 0.0$) shown in Figure 2.

3 RESULTS

3.1 No control case

The flow over an open cavity with a stationary bottom wall is called no control. Instantaneous isosurfaces of spanwise vorticity at $t = 660$ are shown in Figure 3. The vortex sheet of separated shear layer rolls up and a large vortical structure is observed in the upstream region of cavity trailing edge. The vortical structure in the oscillating shear layer is similar to the visualized flow in mode II by Knisely and Rockwell [2] and Gharib and Roshko [4]. Figure 4 shows line integral convolution and velocity vectors in z=0 section. A large clockwise recirculating vortex is observed in the downstream region of the cavity. A secondary counter-rotating week vortex exists in the upstream region of the cavity. The time history of the vertical velocity v at the point A shows almost periodic oscillation behavior in Figure 5. The power spectrum of the vertical velocity at the point A is shown in Figure 6. The horizontal axis represents the non-dimensional frequency. A main peak dominates the spectrum and the Strouhal number based on the cavity depth D is 0.453. The Strouhal number of the no control flow is compared to the experimental data of Knisely and Rockwell [2] in Figure 7. The computational result is in excellent agreement with the experimental data in mode II.

3.2 Control cases

The control method using the moving bottom wall of cavity was applied for the cavity oscillating flow in mode II of shear layer mode. The moving bottom wall velocity u_w was

varied from -0.10 to -1.00. A series of direct numerical simulations for each u_w has been performed. Figure 8 shows the time history of fluctuating vertical velocity v at the point A for several u_w. The control using the moving bottom wall is initiated at t = 660 in the no control case. After the control is turned on, the effect of the moving bottom wall is observed. Figures 8(b) and (c) show that the amplitude of v becomes smaller than that of no control flow, in Figure 8(a), and the effect increases as u_w becomes smaller negative. The amplitude of v for $u_w = -0.34$ is substantially suppressed as shown in Figure 8(d). Further decrease of u_w from -0.34 cause the increase of fluctuating amplitude, as shown in Figures 8(e) and (f). The similar tendency is observed in the time history of fluctuating pressure p at the point A as shown in Figure 9.

Figure 10 and 11 show the effect of the control on statistical characteristics of cavity oscillations. Power spectra of the vertical velocity and the pressure obtained between t = 700 and t = 1060 at the point A are shown in Figure 10 and 11, respectively. The spectra of the no control case are dominated by a spectral peak at the self-sustained oscillating frequency, which is f = 0.453. In the control case for $u_w = -0.34$, the dominant spectral peak at the self-sustained oscillating frequency is strongly attenuated and almost all spectral components are smaller than in the no control case.

Figure 12 shows variations of root-mean-square values of the vertical velocity v and the pressure p at the point A for the moving bottom wall velocity u_w. There is significant effectiveness between $u_w = -0.30$ and $u_w = -0.40$. Being compared with the v rms value 0.111 in the no control flow, the value at $u_w = -0.34$ is 0.0346 and the most reduction is attained. The reduction of 68.8% is achieved for $u_w = -0.34$. A similar result of the p rms value is obtained in Figure 12. For the p rms value, the reduction of 84.2% is achieved with $u_w = -0.34$. The case of $u_w = -0.34$ is optimum in this control method.

The effect of the control method on the vortical structure of the shear layer and the recirculating flow in the cavity is shown in Figure 13. In the no control case of Figure 13(a), a large coherent spanwise vortex is observed in the separated shear layer. In contrast to the no control case, the regular vortex structure is no longer present and the separated shear layer is flat over the cavity for $u_w = -0.34$. It appears that the control method has suppressed self-sustained shear layer oscillations.

Figure 14 shows line integral convolution and velocity vectors in $z = 0.0$ section without and with control. The primary recirculating vortex exists in the downstream half of the cavity and secondary counter rotating vortices are observed near the bottom upstream corner of the cavity in Figure 14(a). For the optimum control case with $u_w = -0.34$, the large-scale clockwise recirculating vortex occupies the whole cavity region due to shear stress of the moving bottom wall.

4 CONCLUSIONS

- Direct numerical simulation was performed for the incompressible flow over an open cavity with a length-to-depth ratio of 2.0 without control. The flow pattern of the

separated shear layer and statistical characteristics indicated mode II oscillation of the shear layer mode.

- The active control using the moving bottom wall of cavity was applied to cavity flow oscillation in direct numerical simulations. The reduction of cavity oscillations be achieved with moving velocity of bottom wall between -0.10 and -1.00.
- The optimum velocity for suppression of cavity oscillations was -0.34 , where the most reduction of both the v rms and the p rms value was achieved.
- For no control case, a main vortex and a secondary vortex existed in the cavity. On the other hand, the main vortex occupied the entire region of cavity for control case due to the shear stress by the moving bottom wall.

ACKNOWLEDGEMENTS

This research was supported by JSPS KAKENHI Grant Number 20560153. This research used computational resources of the HPCI system provided by Osaka University Cyber Media Center through the HPCI System Research Project (Project ID:hp130044).

REFERENCES

[1] Rockwell, D. and Naudascher, E. Review – self-sustaining oscillations of flow pastcavities. *J. Fluid Eng.* (1978) **100**:152-165.
[2] Knisely, C. and Rockwell, D. Self-sustained low-frequency components in an impinging shear layer. *J. Fluid Mech.* (1982) **116**:157-186.
[3] Gharib, M. Response of the cavity shear layer oscillations to external forcing, *AIAA J.* (1987) **25**:43-47.
[4] Gharib, M. and Roshko, A. The effect of flow oscillations on cavity drag. *J. Fluid Mech.* (1987) **177**:501-530.
[5] Rowley, C.W. and Williams, D. R. Dynamics and control of high-Reynolds-number flow over open cavities. *Annu. Rev. Fluid Mech.* (2006) **38**:251-276.
[6] Cattafesta, L.N. et al. Active control of flow-induced cavity oscillations. *Prog. Aero. Sci.* (2008) **44**:479-502.
[7] Yoshida, T. et al. Numerical analysis of control of flow oscillations in open cavity using moving bottom wall. *JSME Inter. J. Series B* (2006) **49**:1098-1104.
[8] Shankar, P.N. and Deshpande, M.D. Fluid mechanics in the driven cavity. *Annu. Rev. Fluid Mech.* (2000) **32**:93-136.
[9] Armfield, S. and Street, R. An analysis and comparison of the time accuracy of fractional-step methods for Navier-Stokes equations on staggered grids, *Inter. J. Num. Meth. Fluids* (2002) **38**:255-282.
[10] Kim, J. and Moin, P. Application of a fractional step method to incompressible Navier-Stokes equations, *J. Comput. Phys.* (1985) **59**:308-323.
[11] Morinishi, Y. et al. Fully conservative finite difference scheme in cylindrical coordinates for incompressible flow simulations, *J. Comput. Phys.* (2004) **197**:686-710.
[12] Rowley, C.W. et al. On self-sustained oscillations in two-dimensional compressible flow over rectangular cavities, *J. Fluid Mech.* (2002) **455**:315-346.

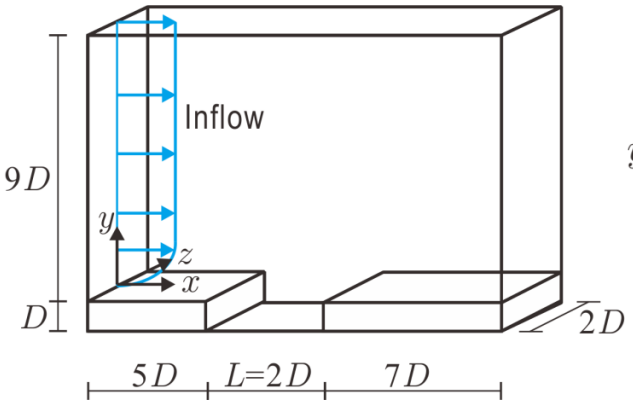

Figure 1: Schematic of the computational domain and the coordinates.

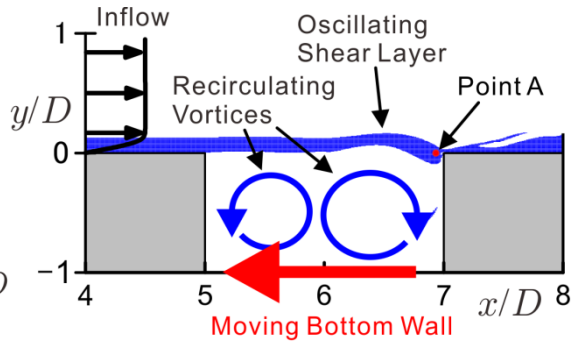

Figure 2: Geometry of the cavity and the control method.

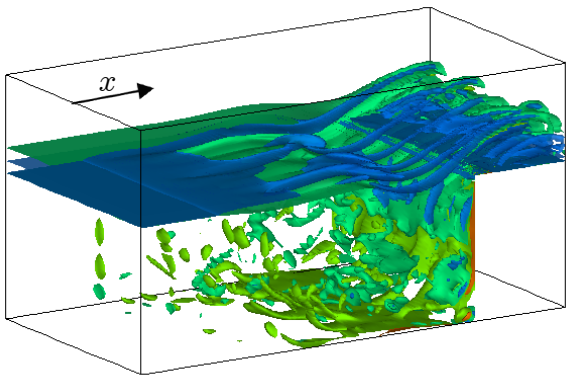

Figure 3: Instantaneous isosurfaces of spanwise vorticity at $t = 660$.

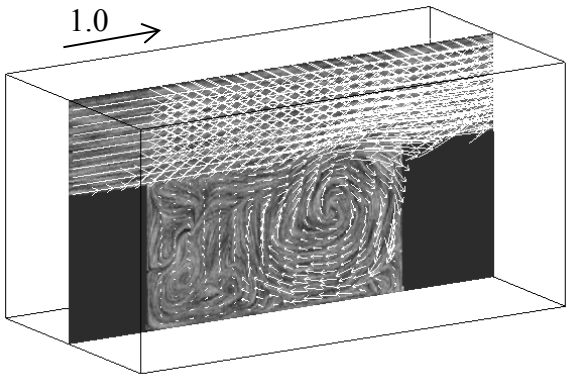

Figure 4: Line integral convolution and velocity vectors in $z = 0.0$ section at $t = 660$.

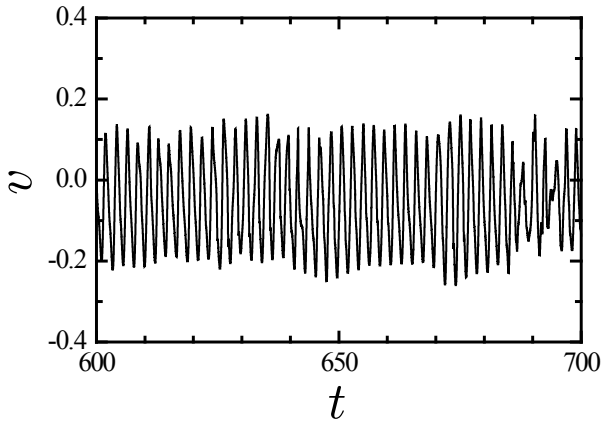

Figure 5: Time history of the vertical velocity at the point A.

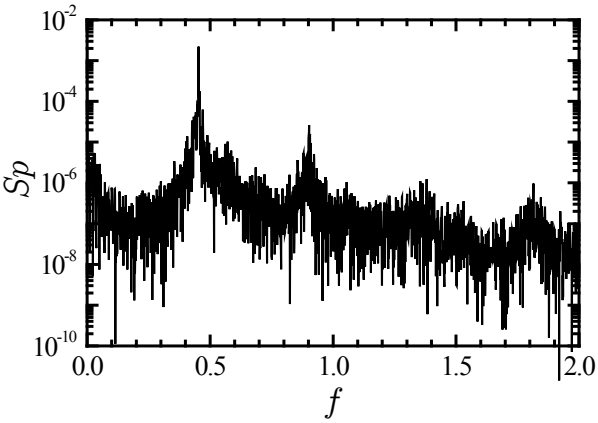

Figure 6: Power spectrum of the vertical velocity at the point A.

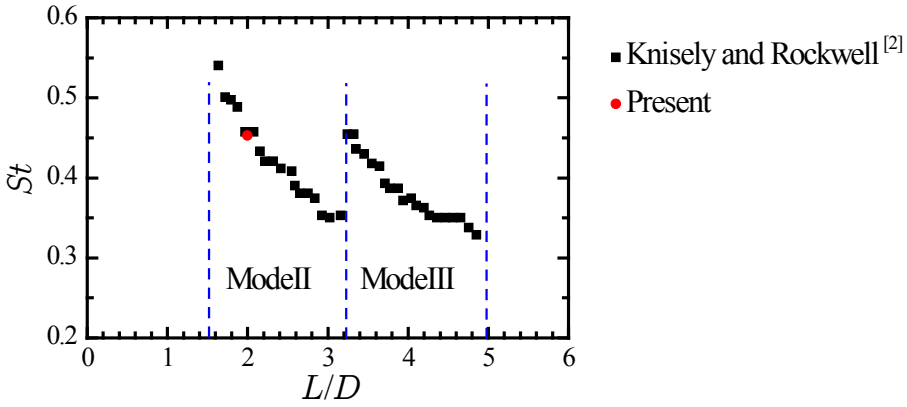

Figure 7: Comparison of Strouhal number with experimental data.

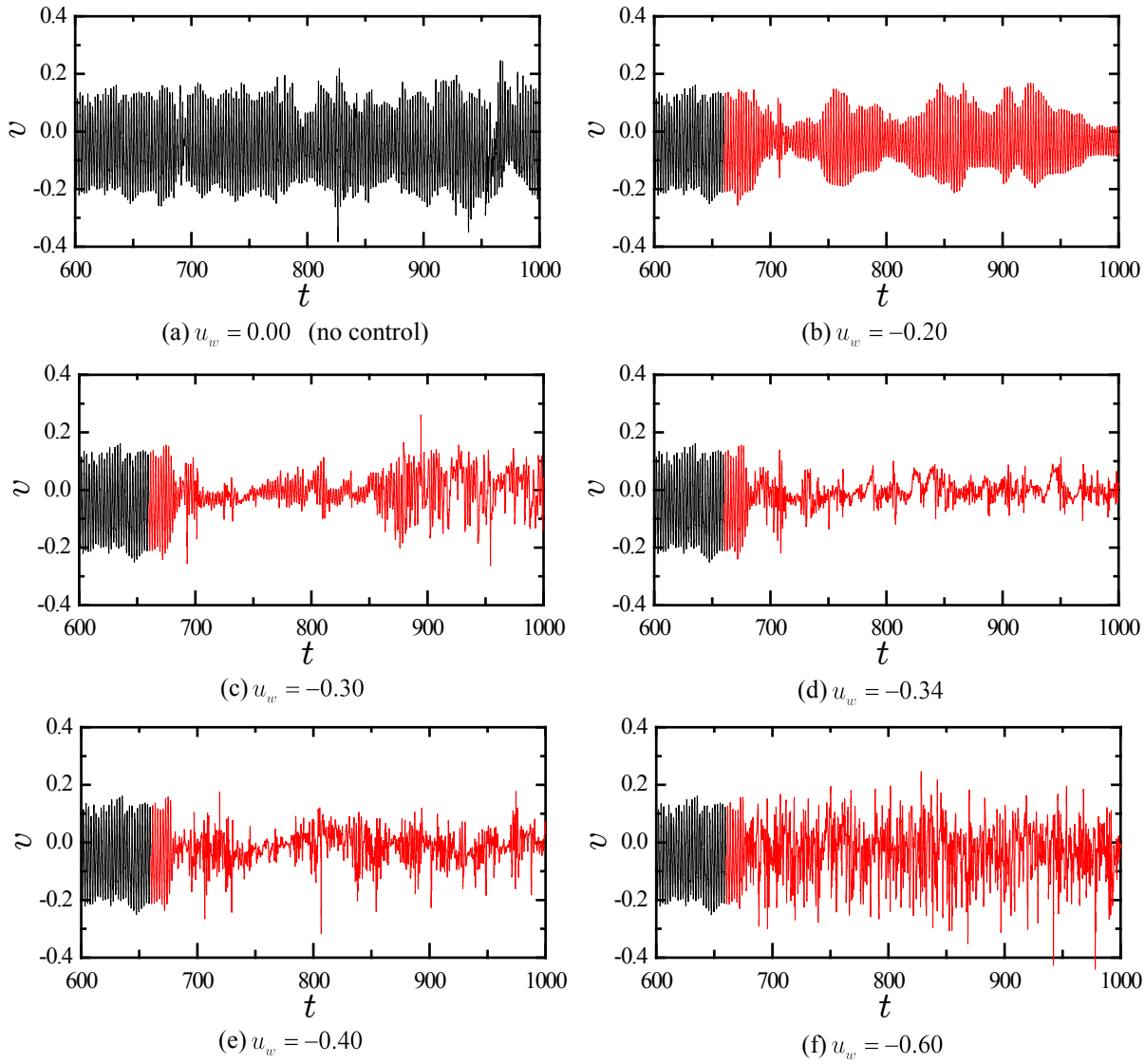

Figure 8:Time history of fluctuating vertical velocity v before and after control that is initiated at $t = 660$.

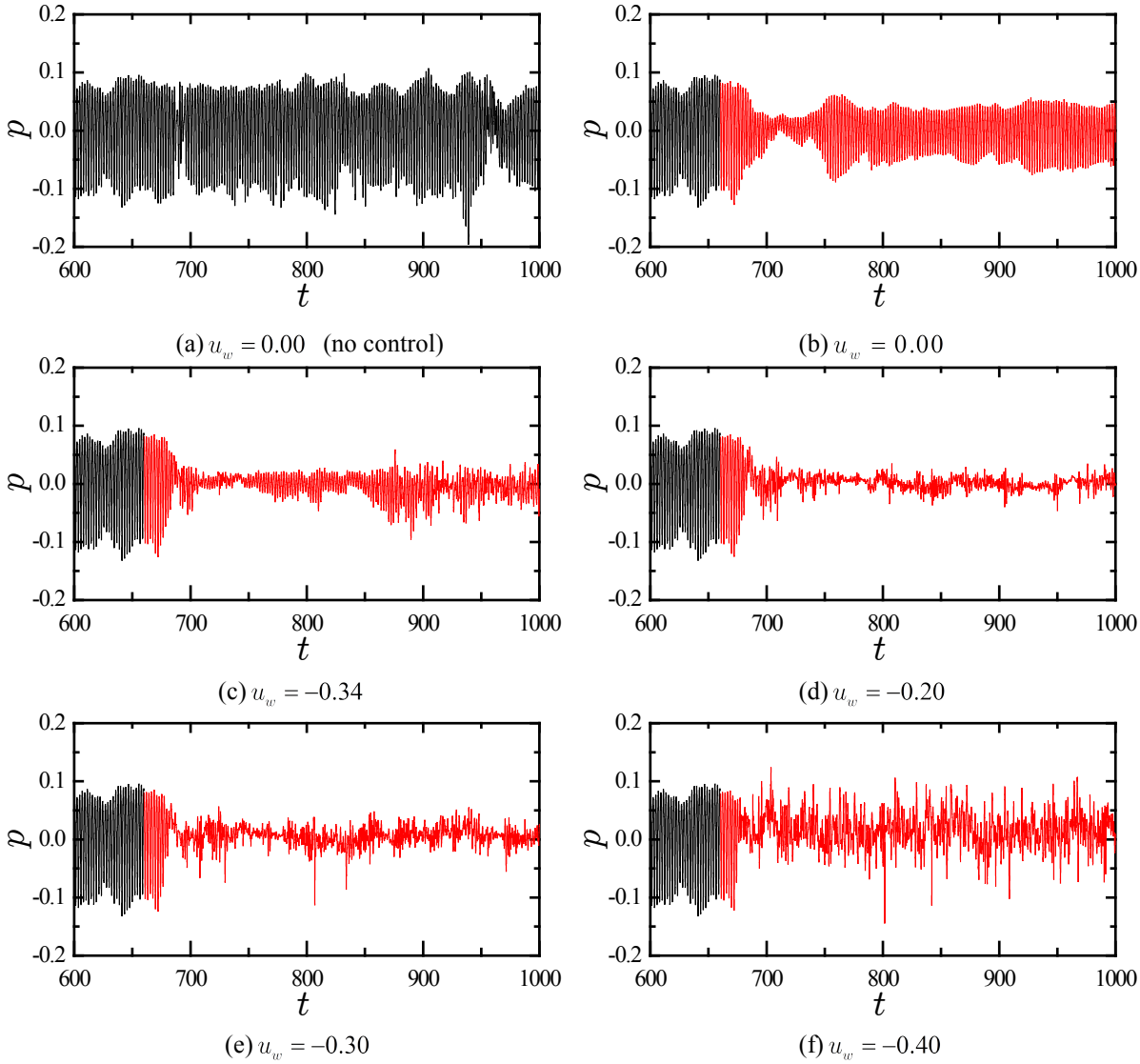

Figure 9:Time history of fluctuating pressure p before and after control that is initiated at $t = 660$.

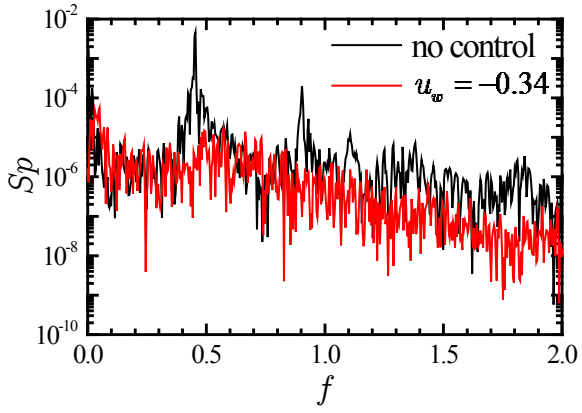

Figure 10: Power specta of the vertical velocity at the point A without and with control.

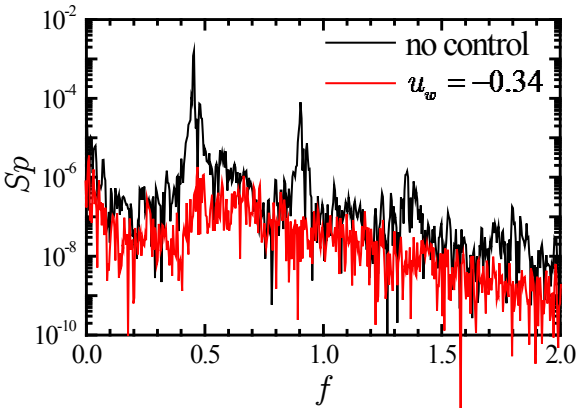

Figure 11: Power specta of the pressure at the point A without and with control.

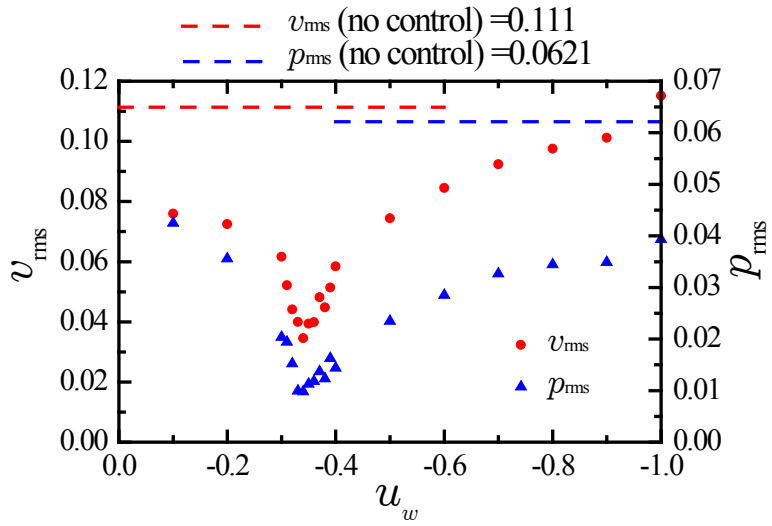

Figure 12: Variation of rms velocity and pressure fluctuations for moving bottom wall velocity.

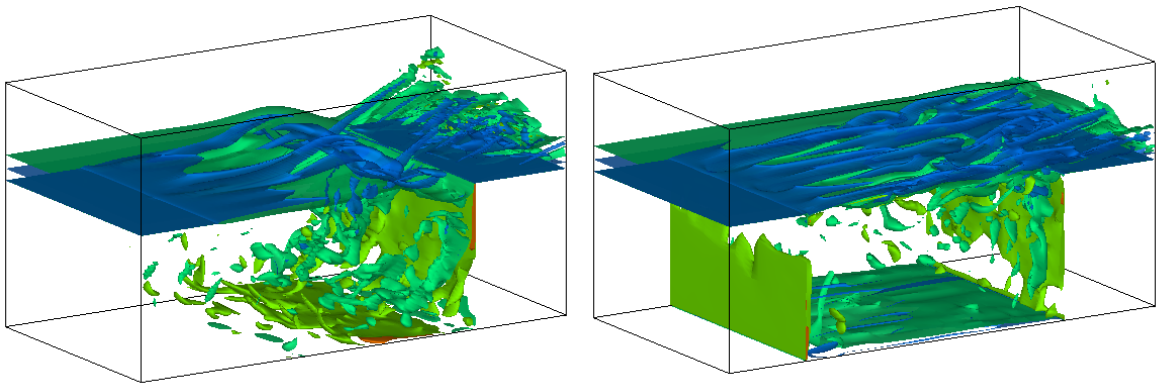

(a) $u_w = 0.00$ (no control) (b) $u_w = -0.34$

Figure 13: Instantaneous isosurfaces of spanwise vorticity at $t = 1060$.

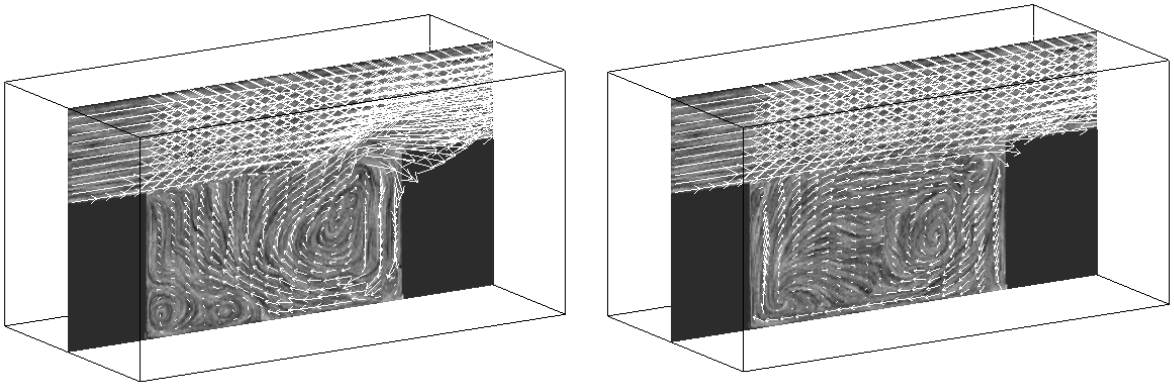

(a) $u_w = 0.00$ (no control) (b) $u_w = -0.34$

Figure 14: Line integral convolution and velocity vectors in $z = 0.0$ section at at $t = 1060$.